Quantum Confinement Drives Macroscopic Stress Oscillations at the Initial Stage of Thin Film Growth

David Flötotto,[1] Zumin Wang,[1,*] Lars P. H. Jeurgens,[1,†] and Eric J. Mittemeijer[1,2]

[1]*Max Planck Institute for Intelligent Systems (formerly Max Planck Institute for Metals Research), Heisenbergstraße 3, D-70569 Stuttgart, Germany*

[2]*Institute for Materials Science, University of Stuttgart, D-70569 Stuttgart, Germany*

(Received 18 April 2012; published 27 July 2012)

Functionalization of thin-film heterostructures on the basis of their electrical, optical and magnetic properties, requires precise control of the film stresses that develop during the growth process. By using real-time *in situ* stress measurements, the present study reveals strikingly that the in-plane film stress *oscillates* with increasing film thickness at the initial stage of epitaxial Al(111) film growth on a Si(111)-$\sqrt{3} \times \sqrt{3}$-Al surface, with a periodicity of 2 times the Fermi wavelength of bulk Al and a stress variation from maximum to minimum as large as 100 MPa. Such macroscopic stress oscillations are shown to be caused by quantum confinement of the free electrons in the ultrathin epitaxial metal film. The amplitude, period, and phase of the observed stress oscillations are consistent with predictions based on the free electron model and continuum elasticity.

DOI: 10.1103/PhysRevLett.109.045501 PACS numbers: 62.25.−g, 68.55.−a, 68.65.−k, 81.15.−z

Epitaxial growth enables the construction of heterostructures of different materials, such as metals, semiconductors and ceramics, with atomic precision [1,2]. Such heterostructures have been the origin of a number of fascinating discoveries in fundamental science (such as the quantum Hall effect in semiconductor heterostructures and the giant magnetoresistance effect in metal heterostructures), and are nowadays widely applied in human life [3,4]. It has long been recognized that a considerable strain/stress can build up during epitaxial growth of heterostructures, as induced by lattice mismatch [5]. The magnitude of the associated growth stress is determined by the difference in the equilibrium lattice spacings of the film and the substrate. Upon increasing the film thickness, the growth stress may partially relax by the formation of misfit dislocations at the heterointerface [6], or by morphological transitions [7,8]. A fundamental understanding of the mechanisms for the generation and relaxation of epitaxial stresses is of vital importance for the controlled reduction of stress-induced defects such as dislocations in heterostructure devices. Furthermore, on this basis a well-controllable strain or stress state can also be induced on purpose to tailor the electronic and optical properties of epitaxial heterostructures [9,10].

In this work it is shown that, surprisingly, the in-plane film stress at the initial stage of (epitaxial) metal film growth *oscillates* with increasing film thickness, with an amplitude as large as hundreds of MPa. Such macroscopic stress oscillations are shown to be driven by the quantum confinement of electrons in the (epitaxial) metal films. This quantum-confinement stress contribution, which has hitherto not been recognized, can play a crucial role in state-of-the-art quantum devices, which, in particular, rely on ultrathin heterostructures. The here discovered direct link between quantum confinement and a macroscopic mechanical property (residual stress) may, in particular, enable the design of novel-concept quantum sensors using mechanical responses.

The experiments were carried out in a multichamber ultrahigh vacuum (UHV) system (base pressure $<1 \times 10^{-8}$ Pa) for thin-film deposition by thermal evaporation and in-vacuo scanning tunneling microscopy (STM). A Si(111)-$\sqrt{3} \times \sqrt{3}$-Al surface was prepared by thermal evaporation of 0.19 monolayer (ML) Al [in this study 1 ML refers to the atomic density of the Al(111) plane at room temperature, i.e. 1 ML = 2.338 Å] at a constant substrate temperature of 700 °C onto a 100-μm thin Si(111) wafer. The Si substrate, which was loosely mounted in the sample holder, had been thoroughly cleaned by a programmed laser heat treatment up to a maximum temperature of 1100 °C for 1 min in UHV. On the thus prepared surface subsequent Al deposition was performed at room temperature. Initially additional 3.7 MLs Al were deposited with a deposition rate of 0.29 ML/min before resuming the Al film growth with a deposition rate of 4.5 ± 0.1 ML/min until a film thickness of 70 nm. The deposition rates employed were calibrated from STM images and by application of a Veeco DekTak profilometer by determing the height of the deposited Al film for a number of deposition times. For a face-centered cubic film with (111) surface orientation the in-plane stress is rotationally symmetric [11]. Stoney's equation [12] was applied to determine the evolution of the thickness-averaged in-plane film stress during deposition from the *in situ* measured substrate curvature as monitored in real time by a multioptical stress sensor (MOS; *k*-space Associates) [13]. The error of the product of thickness-averaged in-plane stress and film thickness is ±0.017 GPa · nm. The film morphology at various stages

of film growth was investigated by STM, with the Si substrate fixed in the sample holder (see supplemental material [14]).

Epitaxial Al film growth on the Si(111)-$\sqrt{3} \times \sqrt{3}$-Al surface takes place by the initial nucleation of monolayer thick Al(111) islands which grow laterally until they coalesce and eventually form a continuous, atomically smooth film (see supplemental material [14] Fig. S1 a–c; cf. Ref. [15,16]). Upon further Al deposition, epitaxial Al film growth proceeds in a step-flow mode (see supplemental material [14] Fig. S1 d–h; cf. Refs. [16,17]), resulting in the formation of a single crystalline Al(111) film with an orientation relationship with the substrate described by Al(111) ∥ Si(111) and Al(110) ∥ Si(110) (see supplemental material [14] Fig. S2). The Al/Si interface is atomically sharp (see supplemental material [14] Fig. S3).

The measured evolution of the average in-plane film stress during epitaxial Al(111) film growth in a thickness range between 5 and 30 ML is shown in Fig. 1(a). The observed average in-plane film stress is compressive and *oscillates* between −225 and −125 MPa during continued epitaxial Al film growth. The amplitude of the stress oscillation becomes attenuated with increasing film thickness. The periodicity of the stress oscillation is about 7.2 Å (3.1 ML), i.e., rather accurately 2 times the bulk Fermi wavelength of Al (2 × 3.6 Å).

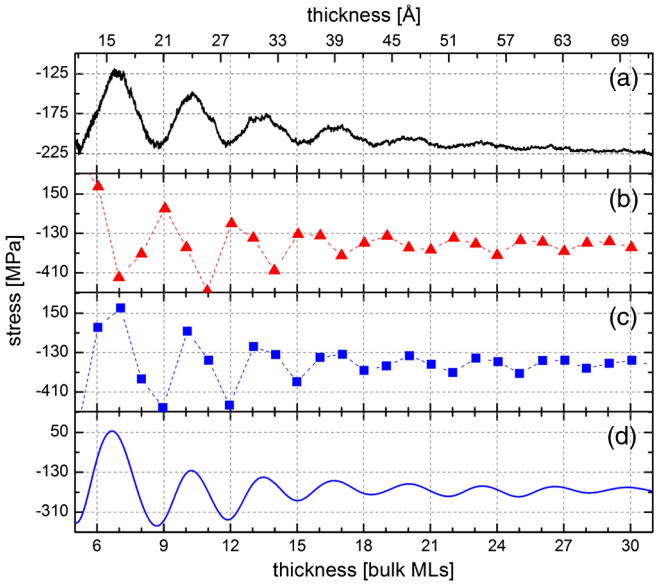

FIG. 1 (color online). (a) Measured evolution of the average in-plane film stress, as function of the film thickness, during epitaxial growth of an Al(111) film on a Si(111)-$\sqrt{3} \times \sqrt{3}$-Al surface. (b) Calculated (according to the recipe shown in Fig. 2 and discussed in the text) average in-plane stress for an Al(111) film of uniform thickness of an integer number of atomic layers, possessing [additionally, as compared to the case considered in Fig. 2(b)] an in-plane growth strain of $\epsilon_{\parallel} = \epsilon_{11} = \epsilon_{22} = -0.0016$. (c) Calculated average in-plane stress, incorporating [additionally to the case considered in (b)] a "phase" (lateral) shift of −0.63 Å (0.27 ML) in $E_{\mathrm{QSE}}(h)$ for an Al(111) film of uniform thickness of an integer number of atomic layers. (d) Calculated average in-plane stress for an Al(111) film incorporating [additionally to the case considered in (c)] the thickness distribution.

The observed step-flow type of growth of the Al film (see above) excludes any morphology effect [18] as the origin of the observed pronounced stress oscillations. As demonstrated in the following, the observed in-plane stress oscillation can be caused by the periodic expansion or contraction of the film, upon overall increasing film thickness, in the direction perpendicular to the film surface, which effect is ascribed to the quantum size effect (QSE) [19,20]: The spatial confinement of electrons in thin metal films results in oscillations of the free electron energy as function of film thickness, with corresponding energy minima occurring at half Fermi wavelength (λ_F) intervals [21]. Therefore the electron energy favors films with thicknesses separated by an integer number of $\lambda_F/2$ and forces thin films with thicknesses of different value to expand or contract perpendicular to the surface. This expansion or contraction is constrained because it is associated with the development of elastic strain energy. As a result of the minimization of the sum of electron energy and strain energy, for a free standing film a geometry emerges with a favored thickness and consequently also preferred lateral dimensions (elastic deformation in the in-plane directions). However, because the lateral dimensions of a thin film attached on a rigid substrate are constrained by the (rigid) substrate, in that case the preferred lateral dimensions cannot be realized and consequently stress components are induced in the plane of the film. The alternation of expansion and contraction of the film thickness upon film growth thus leads to oscillating stress components in the plane of the film. The recipe to calculate the stress component induced by the quantum confinement of the electrons is introduced next.

For a given integer number n of atomic layers film thickness, the instantaneous occurring, equilibrium film thickness, $h_{\mathrm{eq},n}$, is determined by the minimum of the sum of the strain energy per unit film-surface area, $E_{\mathrm{strain}}(h)$, and the excess free electron energy per unit film-surface area due to quantum confinement of the free electrons, $E_{\mathrm{QSE}}(h)$.

$E_{\mathrm{QSE}}(h)$ as function of film thickness h can in principle be calculated using the free electron model for a *freestanding unstrained* Al(111) film with symmetric, infinite energy barriers under the constraint of charge-neutrality requirement (i.e., the negative charge outside the geometrical surfaces equals the electronic charge missing inside the geometrical surfaces; see Ref. [19] and references therein) according to

$$E_{\mathrm{QSE}}(h) = E_{\mathrm{film}}(h) - E_{\mathrm{bulk}} h - 2\gamma^{s}, \qquad (1)$$

where E_{film} is the film energy per unit area, E_{bulk} is the energy per unit volume of the corresponding bulk material

and γ^s is the surface energy. The value of $2\gamma^s$ is given by $[E_{\text{film}}(h) - E_{\text{bulk}}h]_{h\to\infty}$ and thus $E_{\text{QSE}}(h) = 0$ for $h \to \infty$. Using the methodology of Ref. [21], actually E_{QSE} is calculated as function of h, i.e., not for a fixed number of monolayers but for a continuously thickening film (by adding atoms/electrons). The result is shown by the green, dotted curve in Fig. 2(a). Evidently, the calculated E_{QSE} as a function of thickness h resembles a damped sinus function with a periodicity of $\lambda_F/2$. It is supposed that this curve *around the thickness values corresponding to integral numbers of monolayers* provides a realistic estimation for the variations of E_{QSE} as function of h for films composed of such integer numbers of monolayers [solid green curves in Fig. 2(a)].

In the absence of a state of stress, a uniform, thin Al(111) film has a thickness $h_0 = nd^{\infty}_{\text{Al(111)}}$, where $d^{\infty}_{\text{Al(111)}}$ represents the bulk Al(111) interlayer spacing. For the film strained in in-plane and out-of-plane directions (see above discussion), the associated strain energy is given by

$$E_{\text{strain}}(h) = C_{ijkl} \cdot \epsilon_{ij} \cdot \epsilon_{kl} \cdot n \cdot d^{\infty}_{\text{Al(111)}}, \tag{2}$$

where C_{ijkl} is the fourth-rank stiffness tensor as defined in the specimen coordinate system and ϵ_{ij} is the strain tensor

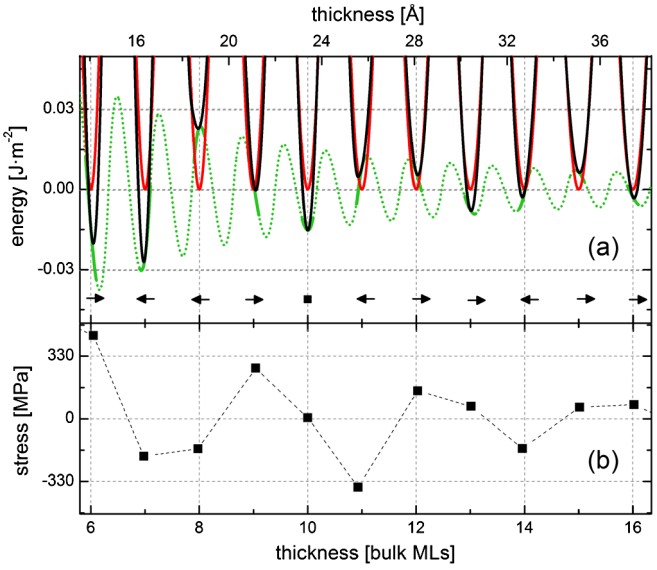

FIG. 2 (color online). (a) The excess electron energy per unit film-surface area due to the quantum confinement of electrons as a function of film thickness (green curve) and the strain energy per unit film-surface area for an uniform film of integer number of atomic layers as function of film thickness (red curves). The minima of the sum curves (black curves = green curve + red curves) determine the instantaneous occurring equilibrium film thickness values for films of integer numbers of atomic layers. The arrows schematically indicate the thickness changes of the films (of integer number of atomic layers) with respect to their h_0 values. (b) The calculated in-plane stress, $\sigma_{\parallel}$, oscillates between tensile and compressive states with overall increasing film thickness.

in the specimen coordinate system. The strain components in this equation are defined with respect to bulk material not subjected to quantum confinement and (lateral) constraints.

For an Al(111) film all shear components of the strain tensors, $\epsilon_{i\neq j}$, are zero and the out-of-plane strain component, ϵ_{33}, is determined by

$$\epsilon_{33} = (h - nd^{\infty}_{\text{Al(111)}})/(nd^{\infty}_{\text{Al(111)}}). \tag{3}$$

In the absence of other source of strain, $\epsilon_{11} = \epsilon_{22} = 0$. Using the values of ϵ_{ij} as indicated, E_{strain} can be calculated as function of h for a film of an integer number of atomic layers; see the red curves in Fig. 2(a). The summations of the individual curves of $E_{\text{QSE}}(h)$ and $E_{\text{strain}}(h)$ are given by the black curves in Fig. 2(a). The minima of these curves then predict the actual, equilibrium thicknesses, $h_{\text{eq},n}$, for films of given integer numbers of atomic layers. The arrows in the figure schematically indicate the thickness changes of the films with respect to the h_0 (see above) values. Using the thus determined values of $h_{\text{eq},n}$, $\epsilon_{33}(h_{\text{eq},n})$ can be calculated from Eq. (3). Next, the (rotationally symmetric) in-plane stress components ($\sigma_{\parallel} = \sigma_{11} = \sigma_{22}$) can be determined from Hooke's law, $\sigma_{ij} = C_{ijkl} \cdot \epsilon_{kl}$, leading to

$$\sigma_{\parallel} = \sigma_{11} = \sigma_{22} = C_{1133}\epsilon_{33}. \tag{4}$$

The resulting values of $\sigma_{\parallel}$ are shown in Fig. 2(b) for increasing film thickness by data points at $h_{\text{eq},n}$. The calculation indeed predicts a damped stress oscillation pattern with overall increasing film thickness. The amplitude of the stress oscillations attenuates with increasing thickness as a consequence of the decrease of the quantum size effect with increasing film thickness. The resulting periodicity of the stress oscillation pattern is a consequence of the interaction of the $d^{\infty}_{\text{Al(111)}}$ periodic minima in $E_{\text{strain}}(h)$ and the $\lambda_F/2$ periodic minima in $E_{\text{QSE}}(h)$. For a Al(111) film the ratio of $\lambda_F/2$ and $d^{\infty}_{\text{Al(111)}}$ is $\approx$ 4:3, which results in a stress oscillation pattern with a periodicity of $\approx 2\lambda_F = 7.2$ Å (3.1 ML), as experimentally observed.

In order to allow comparison of such a prediction of $\sigma_{\parallel}$ oscillation with experimental results, some practical complications have to be taken into account: (i) At (large) thickness values, where the quantum size effect can be ignored, the observed in-plane strain is not equal to zero. For the epitaxial Al film in this study, this in-plane growth strain, $\epsilon_{\parallel} = \epsilon_{11} = \epsilon_{22}$, equals -0.0016, as observed at film thicknesses beyond 30 ML [cf. Fig. 1(a)]. Therefore, in the above sketched calculations, $\epsilon_{\parallel} = 0$ has to be substituted by $\epsilon_{\parallel} = \epsilon_{11} = \epsilon_{22} = -0.0016$. As a result of the accordingly repeated calculation (now using a corresponding modified Eq. (4): $\sigma_{\parallel} = \sigma_{11} = \sigma_{22} = C_{1111}\epsilon_{11} + C_{1122}\epsilon_{22} + C_{1133}\epsilon_{33}$) the overall stress level in the film changes such that the in-plane stress component oscillates around a value of ≈ -220 MPa, instead of around $\sigma_{\parallel} = 0$ [see Fig. 1(b) and compare with Fig. 2(b)]. (ii) The

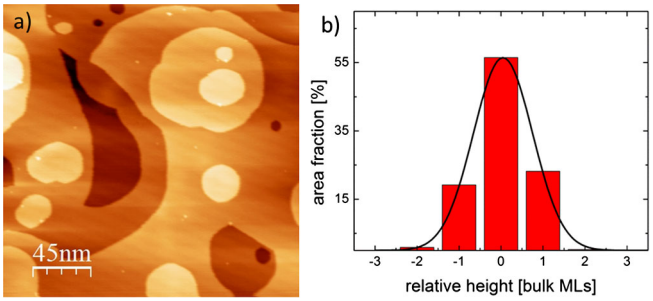

FIG. 3 (color online). (a) STM image (225 nm × 225 nm, specimen bias voltage $V_t = 1.4$ V, tunneling current $I_t = 0.2$ nA) and (b) the corresponding height distribution, after deposition of a nominally 10 nm epitaxial Al film on a Si(111)-$\sqrt{3} \times \sqrt{3}$-Al surface.

"phase" of the stress oscillation pattern strongly depends on the phase of $E_{\mathrm{QSE}}(h)$. Although the periodicity of the oscillation pattern of $E_{\mathrm{QSE}}(h)$ is independent of the used (free) electron model [21,22], the phase of the oscillation pattern of $E_{\mathrm{QSE}}(h)$ distinctly depends on the heights of energy barriers at the substrate/film and film/vacuum interfaces as well as on the lattice potential. Therefore, the present calculation, which is based on the free electron model for a free standing film with equal energy barriers at both film faces, cannot predict exactly the phase of the oscillation pattern of $E_{\mathrm{QSE}}(h)$ [22]. By incorporating a phase (lateral) shift of -0.63 Å (0.27 ML) in $E_{\mathrm{QSE}}(h)$ and then repeating the above sketched calculations, the maxima and minima of the calculated stress oscillation pattern become in perfect agreement with the experimental result [cf. Figs. 1(a) and 1(c)]. (iii) It is recognized that the epitaxially growing Al(111) film exhibits a thickness distribution (see Fig. 3). To consider the effect of the thickness distribution on the average in-plane stress, (a) the percentages of the total film-surface area covered by a film of n atomic layers, p_n, as determined from the STM image at a nominal film thickness of 10 nm, are described by a Gaussian distribution, and (b) it is assumed that the thickness distribution is independent of film thickness (i.e., at all mean film thicknesses the same Gaussian distribution prevails). Then the average in-plane stress $\langle \sigma_{\parallel} \rangle$ at mean film thickness $\langle h \rangle = \sum_{n=1}^{\infty} p_n h_{\mathrm{eq},n}$ is given by

$$\langle \sigma_{\parallel} \rangle = 1/\langle h \rangle \Sigma_{n=1}^{\infty} p_n h_{\mathrm{eq},n} \sigma_{\parallel,n}. \quad (5)$$

The thus calculated curve of average in-plane stress, $\langle \sigma_{\parallel} \rangle$ [i.e., incorporating the effects discussed under (i), (ii), and (iii) above], as function of epitaxial Al(111) film thickness is shown in Fig. 1(d) [note that, because of the effect (iii), this curve now is continuous]. The calculated curve agrees excellently with the measured curve for the average in-plane film stress in terms of the periodicity and the damping behavior [cf. Figs. 1(a) and 1(d)]. The amplitude of the measured stress oscillation is smaller than that of the calculated stress oscillation. This difference can be caused by (1) a broader thickness distribution during film growth as compared to the thickness distribution measured after film growth by STM, and/or (2) elastic constants of ultrathin films which differ from their bulk counterparts [23,24].

In conclusion, macroscopic stress oscillations as large as 100 MPa are observed during the initial stage of epitaxial Al(111) film growth on a Si(111)-$\sqrt{3} \times \sqrt{3}$-Al surface. The stress oscillations are induced by the quantum confinement of electrons in the thin epitaxial metal film. The amplitude, period and phase of the observed macroscopic stress oscillations are consistent with predictions based on the free electron model and continuum elasticity. The here discovered direct link between quantum confinement and macroscopic film stress can play a crucial role for the design of novel-concept functional ultrathin heterostructures.

The authors are grateful to S. Haag for the invaluable discussions, to U. Salzberger for the preparation of the TEM foils, and to Dr. F. Phillipp and Professor L. Gu for the HRTEM investigation.

*Corresponding author.
z.wang@is.mpg.de
†Present address: Swiss Federal Laboratories for Materials Science and Technology, Überlandstrasse 129, 8600 Dübendorf, Switzerland.

[1] W. P. McCray, Nature Nanotech. **2**, 259 (2007).
[2] J. Mannhart and D. G. Schlom, Science **327**, 1607 (2010).
[3] Z. I. Alferov, Rev. Mod. Phys. **73**, 767 (2001).
[4] H. Kroemer, Rev. Mod. Phys. **73**, 783 (2001).
[5] F. C. Frank and J. H. van der Merwe, Proc. R. Soc. A **198**, 216 (1949).
[6] E. A. Fitzgerald, Mater. Sci. Rep. **7**, 87 (1991).
[7] J. A. Floro, E. Chason, R. D. Twesten, R. Q. Hwang, and L. B. Freund, Phys. Rev. Lett. **79**, 3946 (1997).
[8] G. Medeiros-Ribeiro, A. M. Bratkovski, T. I. Kamins, D. A. A. Ohlberg, and R. S. Williams, Science **279**, 353 (1998).
[9] R. S. Jacobsen, K. N. Andersen, P. I. Borel, J. Fage-Pedersen, L. H. Frandsen, O. Hansen, M. Kristensen, A. V. Lavrinenko, G. Moulin, H. Ou, C. Peucheret, B. Zsigri, and A. Bjarklev, Nature (London) **441**, 199 (2006).
[10] A. M. Smith, A. M. Mohs, and S. Nie, Nature Nanotech. **4**, 56 (2008).
[11] L. B. Freund and S. Suresh, *Thin Film Materials: Stress, Defect Formation, and Surface Evolution* (Cambridge University Press, Cambridge, England, 2003).
[12] G. G. Stoney, Proc. R. Soc. A **82**, 172 (1909).
[13] E. Chason and B. W. Sheldon, Surf. Eng. **19**, 387 (2003).
[14] See Supplemental Material at http://link.aps.org/supplemental/10.1103/PhysRevLett.109.045501 for details.
[15] J. Teng, L. Zhang, Y. Jiang, J. Guo, Q. Guo, E. Wang, P. Ebert, T. Sakurai, and K. Wu, J. Chem. Phys. **133**, 014704 (2010).
[16] A. Uemura, A. Ohkita, H. Inaba, S. Hasegawa, and H. Nakashima, and Surf. Sci. **357–358**, 825 (1996)

[17] Y. Horio, Jpn. J. Appl. Phys., Part 1 **38**, 4881 (1999).
[18] D. Sander, S. Ouazi, V. S. Stepanyuk, D. I. Bazhanov, and J. Kirschner, Surf. Sci. **512**, 281 (2002).
[19] Z. Zhang, Q. Niu, and C.-K. Shih, Phys. Rev. Lett. **80**, 5381 (1998).
[20] M. C. Tringides, M. Jałochowski, and E. Bauer, Phys. Today **60**, 50 (2007).
[21] Y. Han and D.-J. Liu, Phys. Rev. B **80**, 155404 (2009).
[22] B. Wu and Z. Zhang, Phys. Rev. B **77**, 035410 (2008).
[23] J.-G. Guo and Y.-P. Zhao, J. Appl. Phys. **98**, 074306 (2005).
[24] F. H. Streitz, R. C. Cammarata, and K. Sieradzki, Phys. Rev. B **49**, 10 699 (1994).